Mesophyll conductance variability of rice aquaporin knockout lines at different growth-stages and growing environments

Xianhong Huang, Zhixin Wang, Jianliang Huang, Shaobing Peng & Dongliang Xiong*

National Key Laboratory of Crop Genetic Improvement, MOA Key Laboratory of Crop Ecophysiology and Farming System in the Middle Reaches of the Yangtze River, College of Plant Science and Technology, Huazhong Agricultural University, Wuhan, Hubei 430070, China

Running head: Mesophyll conductance of the AQP knockout line

Keywords

Mesophyll conductance, photosynthesis, aquaporins, *Ospip1;1, Ospip1;2*, *Ospip2;1,* growth environment

*Corresponding author

Dongliang Xiong

No.1, Shizishan Street , Wuhan, 430070, Hubei, China

Fax: +86-27-87288961

E-mail: dlxiong@mail.hzau.edu.cn

Summary

The plasma membrane subfamily of aquaporins (PIPs) which facilitates the CO_2 diffusion across membranes, is proposed to play an important role in mesophyll conductance to CO_2 (g_m), a major limiting factor of photosynthesis. However, recent studies implied no causal relationship between g_m and PIPs because they were failed to repeat the previous observed differences in g_m between PIP knockout lines and their wild type. The contrasting results on the role of PIPs in g_m were interpreted as the different growth conditions among studies, which has never been tested. Here, we assessed whether the differences in g_m between wild type and PIP knockout lines, *Ospip1;1, Ospip1;2* and *Ospip2;1*, varied with growth condition (field vs pot condition) and growth stages in rice. Under field condition, no differences were observed in plant performance, photosynthetic rate (A) and g_m between PIP knockout lines and the wild type. However, in agreement with previous studies, two of three knockout lines showed significant declines in tiller number, plant height, A and g_m under pot condition. Moreover, we found that the differences in A, and g_m between PIP knockout lines and the wild type varied with the growth stage of the plants. Our results showed that the differences in g_m between PIP knockout lines and wild type were depending on the growth environments and stage of the plants, and further efforts are required to reveal the underlying mechanisms.

Introduction

Mesophyll conductance to CO_2 (g_m), referring to the movement of CO_2 from the intercellular air spaces to the site of carboxylation inside the chloroplast, has been recognized as an important limiting factor of photosynthetic assimilation rate in C_3 plants (Flexas *et al.*, 2012). Over the past decade, g_m has been estimated in hundreds of species, and according to quantitative photosynthetic limitation analysis, it can limit photosynthesis across a range of 25% to 80 % (Gago *et al.*, 2019). The g_m variation across species is linked to the mesophyll structures (reviewed by Evans, 2021), and two of the most important structural traits are mesophyll cell wall thickness and the total chloroplast surface area exposed to mesophyll intercellular air spaces per leaf area. Beyond structural traits, the roles of membrane permeability in regulating g_m, especially under dynamic environmental conditions, have been highlighted recently (Flexas *et al.*, 2006; Xu *et al.*, 2019). Behind each mesophyll cell wall lies the plasma membrane, and chloroplasts in mesophyll cell are enclosed by a double membrane. As these membranes typically contain a diversity of proteins, very limited lipid surface area exists for CO_2 free diffusion, and CO_2 across membranes is then suggested to be regulated by protein pores that are known as aquaporins (AQPs). The plasma membrane intrinsic proteins (PIPs), a subfamily of AQPs, have been demonstrated playing the key role in CO_2 diffusion across membranes (reviewed by Grondin *et al.*, 2016; see refs therein).

The regulation of PIPs on CO_2 across membrane in plant has been widely investigated by previous studies (summarized by Grondin *et al.*, 2016). Some of the studies suggested that single aquaporin-mediated membrane permeability to CO_2 represents a significant proportion of the mesophyll resistance (the reciprocal of g_m) by comparing the g_m values of aquaporin lacking or overexpressed mutants to their wild types. For instance, Arabidopsis mutants lacking *AtPIP1;2* had a 10-fold decline in CO_2 diffusion efficiency across mesophyll plasma membrane compared with the wild type (Heckwolf *et al.*, 2011; Uehlein *et al.*, 2012), and g_m increased near 200% by overexpressing the *OsPIP1;2* in rice (Xu *et al.*, 2019). However, a recent study implied no causal relationship between aquaporins and g_m (Kromdijk *et al.*, 2020). In contrast to the observation in Heckwolf *et al.* (2011) and Uehlein *et al.* (2012), Kromdijk *et al.* (2020) reported no difference of g_m values between AtPIP1:2 knockout line and its wild type by estimating g_m in multiple methods. The reason underlying the different observation in these studies on the role of AtPIP1;2 in g_m is unclear. As proposed in Kromdijk *et al.* (2020) and in Evans (2021), one possibility is

that the growth conditions (light irradiances, photoperiod, temperature) were different in two studies, and the plasticity response of other traits may offset the effect of lacking *AtPIP1;2* in mutants. Indeed, many PIP isoforms exist in Arabidopsis and other species, and the expression patterns of PIP isoforms have been showed to be shaped by growth conditions (Wu et al., 2015). If the target PIP gene does not express under a given growth condition, the PIP knock-out mutants should show no functional difference from the wild type. Another possibility might be the plants were measured in different ontogenetic stages (no information about the estimated leaf and plant age was provided in both studies), as the expression patterns of aquaporins vary with growth stages (Xu *et al.*, 2019).

In addition, although the g_m has been suggested to be important for plant growth and development (see details in Evans, 2021), the growth performance of the PIP knock-out lines was typically evaluated by leaf level photosynthetic measurements which were usually conducted on newly expanded leaves under controlled environment conditions. However, plant growth performance is more closely related to canopy photosynthesis expressing as the sum of the photosynthetic rates of all leaves in the canopy (Terashima and Hikosaka, 1995). The complexity of canopy photosynthesis was frequently described, as the leaves inside canopy are exposed to different environmental conditions, and have different functional traits and ontogeny (Slattery and Ort, 2021; Wu *et al.*, 2019). Therefore, the impacts of PIP genes knock-out on plant performance may better to be evaluated by measuring the growth rather than the photosynthetic rate on newly expanded leaves.

Here, we conducted the study to assess whether the g_m and growth performance of PIP knockout lines are impacted by growth environments and/or growth stage. To do so, we used three rice (*Oryza sativa*) PIP knockout lines that have been reported to be involved in g_m regulation (Ding *et al.*, 2016; Ding *et al.*, 2019; Xu *et al.*, 2019) and the wild type by measuring gas exchange and growth traits under both field and pot conditions, and at three growth stages under pot condition. Rice rather than Arabidopsis was selected in present study because (1) rice is a major staple crop for almost half the global population, and improving g_m and then enhance photosynthesis is proposed to be an important strategy for yield improvement (Long, 2014); (2) compared with Arabidopsis, rice typically has larger leaves which are more favor for gas exchange measurement using commercially available infrared gas analysis systems (discussed in Flexas *et al.*, 2007); and (3) rice, as a crop, has higher photosynthetic rate and stomatal

111 conductance than Arabidopsis, which is important for a precise mesophyll conductance
112 estimation (Gu and Sun, 2014).
113
114

Results

Growth performance

As expected, the plant growth performance differed significantly in two environments. Overall, the plants grown under field condition have less tillers and lower plant height than those grown under pot condition. Importantly, no difference in tiller number between wild type and knockout lines was observed under field condition at Sanya (Figure 1). The average plant heights of the knockout lines were lower than wild type, but only the *Ospip1;1* line was statistically significant. In contrast, both tiller number and plant height of knockout lines were lower than the wild type in pot condition at Wuhan, expect for the plant height of *Ospip1;2* (Figure 2). Moreover, the tiller number and plant height differed significantly among knockout lines in pot condition. The tiller number of *OsPIP1;2* knockout line was almost twice of *OsPIP1;1* knockout line, and the plant height of *OsPIP1;2* knockout line was also higher than that of *OsPIP1;1* knockout line. The difference in tiller number between wild type and PIP knockout lines disappeared at 56 days after sowing, except for the *Ospip1;1* line which had the lowest tiller number and plant height over the growth cycle in pot condition. When comparing the plant performance growing in two conditions, tiller number and plant height of wild type showed larger plasticity than knockout lines, and no plasticity observed for *Ospip1;1* line (Figure 3).

Photosynthetic traits

Overall, the plants grown under field condition had higher photosynthetic rate (A) than those in pots (Figure S4). No differences were observed among plant lines in A and mesophyll conductance (g_m) under field condition (Figure 4). However, the stomatal conductance under field condition differed significantly, that *Ospip1;2* line had the highest g_s and the *Ospip2;1* line had the lowest g_s. The parameters fitted from the light response curves future confirmed that no significant difference in photosynthetic capacity existed among lines under field condition (Figure S5). However, under pot condition, the photosynthetic parameters differed significantly among lines (Figure 4). Similar to the growth performance traits, the *Ospip1;1* had the lowest A over the estimated growth cycle when plants grown up in pots. The differences between knockout lines and the wild type in photosynthetic parameters at ambient CO_2 condition varied with plant growth stages and the net photosynthetic rate tended to decline over the growth cycle. However, according to the CO_2 response curves, we found that the photosynthetic capacities (both V_{cmax}, and J_{max}) of the mutants were similar to the wild type for all three estimated growth

stages (Figure S6-S8). The A, V_{cmax} and J_{max} of the wild type and mutants declined over the growth stages, but the patterns of g_{sw} and g_m were genotype dependent.

Leaf functional traits

Regarding leaf morphological traits, *Ospip1;1* and *Ospip2;1* had smaller leaves at tiller stage, but no difference in flag leaves comparing to the wild type (Table S3). In this study, we also investigated the chemical components, Rubisco content and stable isotopes of carbon for pot growing plants at three growth stages. The results, however, showed that PIP knockout lines had no significant difference from the wild type, except for N content and Rubisco content of *Ospip1;1* at tiller stage (Table S3). Similar to A, the C content, N content and Rubisco content tended to decease over growth stages in all the genotypes, however, the $\delta^{13}C$ increased over the growth stages.

Discussion

Photosynthetic assimilation in C_3 plants under atmospheric condition is typically limited by the CO_2 concentration in chloroplasts, which is determined by the diffusion conductance of CO_2 through boundary layer, stomata and mesophyll tissues (Flexas *et al.*, 2012). As aquaporins are functioning to enhance the permeability of membranes to substances such as water and CO_2, the contribution of aquaporins to CO_2 diffusion conductance, especially to the mesophyll conductance (g_m), have been assessed using mutants in several species (reviewed by Groszmann *et al.*, 2017). Several aquaporin genes were suggested to have a role in CO_2 diffusion across membranes in those studies, however, the results were rarely replicated by other researchers. Most recently, Kromdijk *et al.* (2020) reinvestigated the role of *AtPIP1;2* on g_m in Arabidopsis, and their result, surprisingly, contrasted with previous studies (Heckwolf *et al.*, 2011; Uehlein *et al.*, 2012), which showed strong decline of g_m in *Atpip1;2* mutant comparing to the wild type. Although no empirical data are available, the contrasting results of the role of the aquaporin genes on g_m were proposed to be arisen by the different growth environments and/or the growth stage of the plants (Evans, 2021; Kromdijk *et al.*, 2020). Here, three previous reported g_m-related PIP genes were knocked out to investigate the effects of aquaporin on the plant performances and the g_m under different environments and at different growth stages in rice. We found that the differences in plant growth traits and photosynthetic traits between PIP knockout lines and the wild type were influenced by the growth stage of the plants and the planting conditions.

In rice, eleven PIP genes have been identified, and only the roles of *OsPIP1;1*, *OsPIP1:2* and *OsPIP2;1* in photosynthetic CO_2 diffusion efficiency have been investigated(Ding *et al.*, 2016; Ding *et al.*, 2019; Xu *et al.*, 2019). In this study, the knockout lines of three photosynthesis-associated PIP genes *OsPIP1;1*, *OsPIP1:2* and *OsPIP2;1* were generated using the CRISPR/Cas9 system (Figure S1). Field and pot experiments showed that the plant performance of lines was significantly affected by growth conditions. The tiller number and plant height of plants grown in field condition were much lower than those grown in pot condition except for *Ospip1;1* which had no difference under two conditions. The result agreed with a previous meta-analysis showing that pot-grown plants generally had faster growth rates and different morphology (Poorter *et al.*, 2016). Interestingly, we found that trait plasticity in response to growth environment was strongly affected by PIP genes, as the wild type showed the highest plasticity and the *Ospip1;1* showed no plasticity at all (Figure 3). Although the

mechanisms involving in how PIP genes modulate rice phenotypic plasticity remain to be further revealed, our result suggests that PIP family may play a role in regulating rice phenotypic plasticity induced by environmental changes. While no difference in *A* was observed, the tiller number and plant height were obviously higher in pot growth condition than in field growth condition, indicating the light-saturated leaf level photosynthesis does not predict the whole-plant growth performance of the rice plants.

The *OsPIP1;1* and *OsPIP1;2* were suggested to play an important role in g_m and photosynthesis of rice (Ding *et al.*, 2016; Xu *et al.*, 2019), but the plants lacking of *OsPIP2;1* had no change in g_m in previous studies (Ding *et al.*, 2019). Consistent with the previous study, we found no difference in g_m between the wild type and the *Ospip2;1* line across the investigated growth environment and growth stages. Moreover, we found that the stomatal conductance (g_s) of the *OsPIP2;1* knockout line was lower than the wild type under field condition and pot condition in contrast to the previous study (Ding *et al.*, 2019). The PIP2 type of aquaporin have been suggested to have greater water permeability than the PIP1 type (summarized by Groszmann *et al.*, 2017). In rice, the *PIP2;1* is mainly expressed in endodermis of roots, where aplastic water flow is blocked by hydrophobic substances, and several previous studies have shown that the root hydraulic conductance declined by 80% in the *Ospip2;1* line (Ding *et al.*, 2019; Ishikawa-Sakurai *et al.*, 2017; Sakurai-Ishikawa *et al.*, 2011). Therefore, the declined g_s in *Ospip2;1* might be related to the decreased water transport capacity (plant hydraulics) from root surface to transpiration site inside leaves. Interestingly, the decline in g_s had limited impact on *A*, resulting in a higher water-use efficiency (WUE). The result indicated that the stomatal pores were over-open at normal conditions, as observed in the previous study (Caine *et al.*, 2019). Therefore, decreasing the g_s by mutating of *OsPIP2;1* might be a potential way to enhance WUE of paddy field rice which consume up to 90% of the total water used for irrigation in Asia (Khepar *et al.*, 2000).

Unlike the *OsPIP2;1*, here we observed that the influences of *OsPIP1;1* and *OsPIP1;2* on *A* and g_m were depending on the growth conditions and the growth stages of the plants. Given the high homology of aquaporin isoforms in rice, the compensation between different aquaporin isoforms to mask effects of single gene loss would be expected. If this is the case, the question becomes why the compensation effect differs with growth conditions. By combination of biochemical and cellular biology techniques, the aquaporin activities have been confirmed to be

regulated by post-translational modifications and protein interactions (reviewed by Chaumont and Tyerman, 2014). Plants perceive and process environmental simulation signals by plasma membrane receptor-like protein kinases (RLKs), which comprise a major gene family in plant with over 1131 members in rice (Shiu *et al.*, 2004). Previous studies have demonstrated that the activities of aquaporins are regulated by RLKs, and a given RLK may regulate some specific aquaporins (Grison *et al.*, 2019; Rodrigues *et al.*, 2017; Wu *et al.*, 2015). For instance, Wu *et al.* (2015) reported that the activities of *OsPIP1;1, OsPIP1;3* and *OsPIP2;3* are regulated by *LP2*, a leucine rich repeat RLK member, in responding to soil water change. Indeed, the climate of the rice growing season in Sanya was warming (over the growth season, the maximum air temperature, the minimum air temperature and the average air temperature were 28.5 ^{o}C, 12 ^{o}C, 21.5 ^{o}C, respectively), cloudy and moist; but the climate in Wuhan was hot (over the growth season, the maximum air temperature, the minimum air temperature and the average air temperature 37.5 ^{o}C, 15.8 ^{o}C, 26.5 ^{o}C, respectively), sunny and dry. Therefore, different RLKs may express in two growth conditions, and the RLK-dependent modulation of aquaporin activities might correspond to the variable functional performances in different growth conditions as well as different growth stages. Although future investigations required, the lower g_m values of wild type as well as the knock-out lines growing in pots than the ones growing in field conditions might relate to the interactions between PIPs and RLKs. It is worthy of note that leaf morphological and biochemical traits differed between plants grown in field and pot conditions, which could also contribute to the difference in physiological traits. Moreover, the highly dynamic expression pattern of aquaporin genes may also play a role in the variable functional performances at different growth stages (Sakurai *et al.*, 2005; Xu *et al.*, 2019).

Photosynthetic traits are complex because they are affected by many structural, biochemical and physiological traits (Flexas *et al.*, 2012; Xiong and Flexas, 2018; Xiong and Nadal, 2020). In fact, the leaf area and Rubisco content varied significantly over the growth stages as well as among lines, and those modifications could have impact on photosynthetic performance. Similar to OsPIP2;1, both OsPIP1;1 and OsPIP1;2 have been reported to act as water channels (Liu *et al.*, 2007; Liu *et al.*, 2013; Yu *et al.*, 2006), and, therefore, they may play a role in plant hydraulic conductance. Plant hydraulic conductance is an important determinant of photosynthesis because it sets up the maximum g_s (Brodribb *et al.*, 2007). In fact, the g_s values of *Ospip1;1* was significantly lower than the wild type over the growing season in pot condition. In

addition, g_s values for plant growing in field condition were much lower than that in the pot condition. As the coordination of plant hydraulic conductance, g_s and g_m (Flexas *et al.*, 2013; Xiong *et al.*, 2017), the differences between knockout lines and the wild type in photosynthetic parameters over the growth conditions and growth stages might be related to the aquaporins mediated plant hydraulic conductance adjustment.

Experimental procedures

OsPIP1;1, *OsPIP1;2* and *OsPIP2;1* knockout line creation

Sequences of three rice PIP genes, *OsPIP1;1*, *OsPIP1;2* and *OsPIP2;1*, were obtained from Rice Genome Annotation Project (http://rice.plantbiology.msu.edu/) for CRISPR/Cas9 targets design. Two targets for each gene were designed using the tool CRISPR-GE (https://skl.scau.edu.cn). All the target sequences were listed in Table S1. For each construct, the synthesized oligonucleotide fragments were introduced into tRNA intron and sgRNA expression cassette, driven by OsU3 promoter, in the Y1 vector (from Biorun bio-technology co. Ltd. Wuhan, China), respectively. Then the two targets expression cassettes were then ligated to one vector based on Golden Gate cloning. The CRISPR/Cas9 constructs were then introduced into *Agrobacterium tumefaciens* strain EHA105 after verified by sequencing, which were separately transferred into the rice cultivar *Nipponbare* background by Agrobacterium-mediated transformation. The transgenic lines (T_0) were transplanted into the 10 L pots and grown up in a growth chamber (Conviron, Controlled Environments Limited, Manitoba, Canada) with a 12 h light/12h dark cycle at 25–28 ^{o}C. Genomic DNA was extracted from transformant seedlings for PCR using specific primers (Table S2). Mutations in the PCR products were detected through direct Sanger sequencing method. Next, the PCR products were identified by comparing sequences to the Nipponbare reference using the online tool--DSDecode (http://skl.scau.edu.cn/dsdecode/). The progenies of the plants which are biallelic mutation (Figure S1) of each gene were screened out, and the seeds from the T_1 generation plants were used in the current research after verified with genotyping.

Growth condition

A field and a pot experiments were conducted to investigate the influences of growth environments on photosynthetic and growth performance. The field experiment was carried out at Sanya, Hainan between November 2019 and February 2020. The average temperature and relative humidity in Sanya was 21.5 ^{o}C and 79.9%, respectively, during the experiment. Seeds were germinated and grown in seedling trays for 10 days, and then the seedlings were transplanted to the paddy field in a randomized block design. The field management, nutrient, and irrigation followed local practices. The pot experiment was conducted at Huazhong Agricultural University (HZAU, Wuhan, China) between August to November 2020. The average temperature in Wuhan was 26.5 ^{o}C, while the relative humidity (80.46%) was similar to that in Sanya during the experiment. Seeds were also germinated and grown in seedling tray for

10 days prior to transferring into 13 L plastic pots containing 10 kg of soil applying with 10.0 g of compound fertilizer (N: P_2O_5: K_2O = 1: 1: 1). In each pot, a mutant seedling was planted in pair with a wild-type seedling. Plants were grown outdoors, and the pots were rearranged weekly to avoid edge effects. The photosynthetic performances at the different growth stage were only investigated in the pot experiment, as to have the gas exchange measured precisely in paddy field conditions is quite difficult (Du *et al.*, 2020).

Gas exchange and chlorophyll fluorescence measurements

Gas exchange and chlorophyll fluorescence parameters were measured on newly and fully expanded leaves using a LI-6800 portable photosynthesis system (LI-COR Inc., Lincoln, NE, USA). Thirty-three days after sowing, the light response curves were measured on newly and fully expanded leaves of plants growing in the paddy field. The leaf temperature in the gas exchange chamber was set to 30 ^{o}C, the reference CO_2 concentration was set to 400 μmol mol^{-1}, and the VPD was set to 1.5 kPa. Leaves were firstly acclimated at the PPFD of 1500 μmol m^{-2} s^{-1} and then the auto-progress of light response curve was adopted. The PPFD were set to 1500, 800, 600, 200, and 0 μmol m^{-2} s^{-1} in a serial with the interval of 60-90 s. Measurements were conducted between 9:00am and 15:00 pm. For each measurement, the gas exchange parameters, steady-state fluorescence (F'_s), and maximum fluorescence (F'_m) were recorded, simultaneously.

The gas exchange and chlorophyll fluorescence in the pot experiment were measured in a growth chamber (Conviron, Controlled Environments Limited, Manitoba, Canada), where the air temperature was 28 ± 5 ^{o}C, the PPFD was set to 1500 μmol m^{-2} s^{-1} using a lab-made LED light source, and relative humidity was about 60%. One day before the measurements were performed, pots were moved into the growth chamber. Gas exchange and chlorophyll fluorescence parameters were measured at 39, 57 and 66 days after sowing, respectively. The environmental conditions inside the gas exchange system were set as described above. After the leaf reached a steady state (the fluctuation of stomatal conductance - g_s - being less than 0.05 mol m^{-2} s^{-1} during a 10-min period) the auto-progress of CO_2 response curve was adopted. The reference CO_2 concentrations were subsequently set at 400, 300, 200, 100, 50, 400, 600, 800, 1000, 1200, 1500, 2000, 400 μmol CO_2 mol^{-1} air. The CO_2 response curve measurements were performed between 8:30 am and 17:00 pm each day.

The actual photochemical efficiency of photosystem II (Φ_{PSII}) was calculated as:

$$\Phi_{PSII} = \frac{(F_m' - F_s)}{F_m'}$$

The electron transport rates (J) were computed as follows:

$$J = \Phi_{PSII} \cdot \mathrm{PPFD} \cdot \alpha\beta$$

Where α and β are the leaf absorption and the distribution of electrons between photosystem I and photosystem II, respectively. The αβ was determined from the slope of the relationship between Φ_{PSII} and the quantum efficiency of CO_2 uptake (Figure S2), which was obtained by varying light intensity under non-photorespiratory conditions at less than 2% O_2 (Valentini *et al.*, 1995; Yin *et al.*, 2009).

The mesophyll conductance of CO_2 (g_m) was calculated based on the variable J method described by Harley *et al.* (1992), as follows:

$$g_m = \frac{A}{C_i - \frac{\Gamma^*\left(J + 8\left(A + R_d\right)\right)}{J - 4\left(A + R_d\right)}}$$

where A is net rate of CO_2 assimilation, C_i is the intercellular CO_2 concentration, and Γ* is the CO_2 compensation point in the absence of respiration, R_d is the day respiration. In the present study, a Γ* value of 40 μmol $mol^{-1}$and Rd value of 1 μmol m^{-2} s^{-1}, which were typical for rice plants, were adopted (Xiong *et al.*, 2017; Xiong and Flexas, 2018). Maximum carboxylation rate (V_{cmax}), maximum electron transport rate (J_{max}) were estimated from A-C_i curves using *plantecophys* package (Duursma, 2015).

In the current study, the g_m of pot growing plants was also estimated by using the CO_2 response curve-fitting method, and the relationship between two estimates of gm was shown in Figure S3. As the g_m values from both methods were very similar, we used the values obtained by the variable J method to compare with other parameters.

Plant growth and leaf morphology

Plant height (cm) measured from ground level to the tip of the longest leaf, tiller number were counted for PIP knock-out lines and the wild type. For the field experiment, plant height and tiller number were measured at the 43rd day after sowing. Plant height and the tiller number were investigated at the 39th, 57th and 66th days after sowing under pot condition. To have leaf morphological traits measured, leaves were scanned and then the leaf width, leaf length and area were manually done in an open-source Java image processing program, ImageJ

(https://imagej.net).

Leaf N, C, $\Delta^{13}C$ and Rubisco content

Leaf disks of known area were collected after the gas exchange measurement and then oven dried at 80 °C for 72 hours. Dry samples were grounded before leaf chemical component and the carbon isotope measured using an Isotope ratio mass spectrometry (IRMS; IsoPrime 100 IRMS, Isoprime Ltd, Stockport, UK). The Rubisco content of newly expanded leaves was measured using the SDS–PAGE (sodium dodecyl sulphate–polyacrylamide gel electrophoresis) method. Leaf tissues for Rubisco concentration measurement were immersed in liquid nitrogen and then stored at -80 °C before measuring. The frozen leaf sample was ground with liquid nitrogen on ice and homogenized in an extraction buffer [50 mM Tris-HCl (pH 8.0), 5 mM β-mercaptoethanol and 12.5% (v/v) glycerol]. After centrifugation (15000 rpm, 15 min, 4 °C), 0.5 ml supernatant solution was separated and then 0.5 ml dissolving buffer containing 2% (w/v) SDS, 4% (v/v) β-mercaptoethanol and 10% (v/v) glycerol was added. The Rubisco samples were loaded onto SDS-PAGE containing a 12.5% (w/v) polyacrylamide gel. After electrophoresis, the gels were washed with deionized water several times and then dyed in 0.25% (w/v) Coomassie blue staining solution (Coomassie dissolved in the buffer with water: ethanol: acetic acid=5:4:1) for 12 h and decolorized (in the buffer with water: ethanol: acetic acid = 5:4:1) until the background was colorless. The washed solutions were measured at 595 nm (Infinite M200, Tecan U.S., Inc) using the background glue as a blank.

Data analysis

Light response curve parameters, including the maximum net photosynthetic rate (A_{sat}), light compensation point (LCP) and PPFD at the 75% saturation photosynthetic rate (LSP) were fitted using the nonrectangular hyperbola–based model.

$$A = \frac{\Phi \times \mathrm{PPFD} + A_{\mathrm{gmax}} - \sqrt{(\Phi \times \mathrm{PPFD} + A_{\mathrm{gmax}})^2 - 4\theta \times \Phi \times \mathrm{PPFD} \times A_{\mathrm{gmax}}}}{2\theta} - R_{\mathrm{n}}$$

where Φ is the quantum yield at PPFD = 0 μmol (photon) m^{-2} s^{-1}, A_{gmax} is the maximum gross photosynthetic rate, θ is the convexity factor, and R_n is dark respiration. The model was fitted to the data using the Orthogonal Nonlinear Least-Squares Regression (*onls*) function. Statistical

379 analysis performed using packages of *agricolae*. Other analyses and plots were conducted using
380 the *tidyverse* package. All analyses were performed in R 3.6.3 platform.
381
382 **Data Availability Statement**
383 All relevant data supporting the results presented in this work are available within the article and
384 the supporting materials.
385
386 **Acknowledgements**
387 This study was supported by the National Natural Science Foundation of China (No.
388 32022060) and the National Key Research and Development Program of China (No.
389 2016YFD0300210).
390
391 **Author contribution**
392 DX designed the research; XH and ZW performed the experiments; XH and DX analyzed
393 data; and DX wrote the paper with inputs from all the authors.
394
395 **Conflict of Interest**
396 The authors declare that they have no conflicts of interest associated with this work.
397
398
399 **Supporting information**
400
401 **Table S1.** Designed targets for the three *OsPIP* genes.
402
403 **Table S2.** Primers used for the CRISPR/Cas9 mutant identification.
404
405 **Table S3**. Leaf morphological and biochemical features at different growth stages.
406
407 **Figure S1**. Identification of the O*spip* mutants in T_0 CRISPR/Cas9 edited plants.
408
409 **Figure S2**. Calibration relationship *A* versus PPFD $\Phi_{PSII}/4$ measured under nonphotorespiratory

conditions.

Figure S3. Correlation between mesophyll conductance (g_m) fitted by *Either method* and mesophyll conductance (g_m) calculated by variable *J* methods.

Figure S4. Gas exchange traits varied between plants grown under field and pot conditions.

Figure S5. Light response curves of wild type and *OsPIP* knockout lines.

Figure S7. CO_2 response curves of wild type and *OsPIP* knockout lines at the 39th day after sowing.

Figure S8. CO_2 response curves of wild type and *OsPIP* knockout lines at the 57th day after sowing.

References

Brodribb, T.J., Feild, T.S. and Jordan, G.J. (2007) Leaf maximum photosynthetic rate and venation are linked by hydraulics. *Plant Physiology*, 144, 1890–1898.

Caine, R.S., Yin, X., Sloan, J., Harrison, E.L., Mohammed, U., Fulton, T., Biswal, A.K., Dionora, J., Chater, C.C., Coe, R.A., Bandyopadhyay, A., Murchie, E.H., Swarup, R., Quick, W.P. and Gray, J.E. (2019) Rice with reduced stomatal density conserves water and has improved drought tolerance under future climate conditions. *New Phytologist*, 221, 371–384.

Chaumont, F. and Tyerman, S.D. (2014) Aquaporins: highly regulated channels controlling plant water relations. *Plant Physiology*, 164, 1600–1618.

Ding, L., Gao, L., Liu, W., Wang, M., Gu, M., Ren, B., Xu, G., Shen, Q. and Guo, S. (2016) Aquaporin plays an important role in mediating chloroplastic CO_2 concentration under high-N supply in rice (*Oryza sativa*) plants. *Physiologia Plantarum*, 156, 215–226.

Ding, L., Uehlein, N., Kaldenhoff, R., Guo, S., Zhu, Y. and Kai, L. (2019) Aquaporin PIP2;1 affects water transport and root growth in rice (*Oryza sativa* L.). *Plant Physiology and Biochemistry*, 139, 152–160.

Du, T., Meng, P., Huang, J., Peng, S. and Xiong, D. (2020) Fast photosynthesis measurements for phenotyping photosynthetic capacity of rice. *Plant methods*, 16, 6.

Duursma, R.A. (2015) Plantecophys--An R package for analysing and modelling leaf gas exchange data. *PloS one*, 10, e0143346.

Evans, J.R. (2021) Mesophyll conductance: walls, membranes and spatial complexity. *New Phytologist*, 229, 1864–1876.

Flexas, J., Barbour, M.M., Brendel, O., Cabrera, H.M., Carriquí, M., Díaz-Espejo, A., Douthe, C., Dreyer, E., Ferrio, J.P., Gago, J., Gallé, A., Galmés, J., Kodama, N., Medrano, H., Niinemets, Ü., Peguero-Pina, J.J., Pou, A., Ribas-Carbó, M., Tomás, M., Tosens, T. and Warren, C.R. (2012) Mesophyll diffusion conductance to CO_2: an unappreciated central player in photosynthesis. *Plant Science*, 193-194, 70–84.

Flexas, J., Ortuño, M.F., Ribas-Carbo, M., Diaz-Espejo, A., Flórez-Sarasa, I.D. and Medrano, H. (2007) Mesophyll conductance to CO_2 in *Arabidopsis thaliana*. *New Phytologist*, 175, 501–511.

Flexas, J., Ribas-Carbó, M., Hanson, D.T., Bota, J., Otto, B., Cifre, J., McDowell, N., Medrano, H. and Kaldenhoff, R. (2006) Tobacco aquaporin NtAQP1 is involved in mesophyll conductance to CO_2 *in vivo*. *Plant Journal*, 48, 427–439.

Flexas, J., Scoffoni, C., Gago, J. and Sack, L. (2013) Leaf mesophyll conductance and leaf hydraulic conductance: an introduction to their measurement and coordination. *Journal of Experimental Botany*, 64, 3965–3981.

Gago, J., Carriquí, M., Nadal, M., Clemente-Moreno, M.J., Coopman, R.E., Fernie, A.R. and Flexas, J. (2019) Photosynthesis optimized across land plant phylogeny. *Trends in Plant Science*, 24, 947–958.

Grison, M.S., Kirk, P., Brault, M.L., Wu, X.N., Schulze, W.X., Benitez-Alfonso, Y., Immel, F. and Bayer, E.M. (2019) Plasma membrane-associated receptor-like kinases relocalize to plasmodesmata in response to osmotic stress. *Plant Physiology*, 181, 142–160.

Grondin, A., Mauleon, R., Vadez, V. and Henry, A. (2016) Root aquaporins contribute to whole plant water fluxes under drought stress in rice (*Oryza sativa* L.). *Plant, Cell & Environment*, 39, 347–365.

Gu, L. and Sun, Y. (2014) Artefactual responses of mesophyll conductance to CO_2 and

irradiance estimated with the variable J and online isotope discrimination methods. *Plant, Cell & Environment*, 37, 1231–1249.

Harley, P.C., Loreto, F., Di Marco, G. and Sharkey, T.D. (1992) Theoretical considerations when estimating the mesophyll conductance to CO_2 flux by analysis of the response of photosynthesis to CO_2. *Plant Physiology*, 98, 1429–1436.

Heckwolf, M., Pater, D., Hanson, D.T. and Kaldenhoff, R. (2011) The Arabidopsis thaliana aquaporin AtPIP1;2 is a physiologically relevant CO_2 transport facilitator. *Plant Journal*, 67, 795–804.

Ishikawa-Sakurai, J., Murai-Hatano, M., Hayashi, H., Matsunami, M. and Kuwagata, T. (2017) Rice aquaporins and their responses to environmental stress. *Root Research*, 26, 39–55.

Khepar, S.D., Yadav, A.K., Sondhi, S.K. and Siag, M. (2000) Water balance model for paddy fields under intermittent irrigation practices. *Irrig Sci*, 19, 199–208.

Kromdijk, J., Głowacka, K. and Long, S.P. (2020) Photosynthetic efficiency and mesophyll conductance are unaffected in *Arabidopsis thaliana* aquaporin knock-out lines. *Journal of Experimental Botany*, 71, 318–329.

Liu, C., Fukumoto, T., Matsumoto, T., Gena, P., Frascaria, D., Kaneko, T., Katsuhara, M., Zhong, S., Sun, X., Zhu, Y., Iwasaki, I., Ding, X., Calamita, G. and Kitagawa, Y. (2013) Aquaporin OsPIP1;1 promotes rice salt resistance and seed germination. *Plant Physiology and Biochemistry*, 63, 151–158.

Liu, H.-Y., Yu, X., Cui, D.-Y., Sun, M.-H., Sun, W.-N., Tang, Z.-C., Kwak, S.-S. and Su, W.-A. (2007) The role of water channel proteins and nitric oxide signaling in rice seed germination. *Cell Research*, 17, 638–649.

Long, S.P. (2014) We need winners in the race to increase photosynthesis in rice, whether from conventional breeding, biotechnology or both. *Plant, Cell & Environment*, 37, 19–21.

Poorter, H., Fiorani, F., Pieruschka, R., Wojciechowski, T., van der Putten, W.H., Kleyer, M., Schurr, U. and Postma, J. (2016) Pampered inside, pestered outside? Differences and similarities between plants growing in controlled conditions and in the field. *New Phytologist*, 212, 838–855.

Rodrigues, O., Reshetnyak, G., Grondin, A., Saijo, Y., Leonhardt, N., Maurel, C. and Verdoucq, L. (2017) Aquaporins facilitate hydrogen peroxide entry into guard cells to mediate ABA- and pathogen-triggered stomatal closure. *Proceedings of the National Academy of Sciences of the United States of America*, 114, 9200–9205.

Sakurai, J., Ishikawa, F., Yamaguchi, T., Uemura, M. and Maeshima, M. (2005) Identification of 33 rice aquaporin genes and analysis of their expression and function. *Plant & Cell Physiology*, 46, 1568–1577.

Sakurai-Ishikawa, J., Murai-Hatano, M., Hayashi, H., Ahamed, A., Fukushi, K., Matsumoto, T. and Kitagawa, Y. (2011) Transpiration from shoots triggers diurnal changes in root aquaporin expression. *Plant, Cell & Environment*, 34, 1150–1163.

Shiu, S., Karlowski, W.M., Pan, R., Tzeng, Y., Mayer, K.F.X. and Li, W. (2004) Comparative analysis of the receptor-like kinase family in Arabidopsis and rice. *Plant Cell*, 16, 1220–1234.

Slattery, R.A. and Ort, D.R. (2021) Perspectives on improving light distribution and light use efficiency in crop canopies. *Plant Physiology*, 185, 34–48.

Terashima, I. and Hikosaka, K. (1995) Comparative ecophysiology of leaf and canopy photosynthesis. *Plant, Cell & Environment*, 18, 1111–1128.

Uehlein, N., Sperling, H., Heckwolf, M. and Kaldenhoff, R. (2012) The *Arabidopsis* aquaporin PIP1;2 rules cellular CO_2 uptake. *Plant, Cell & Environment*, 35, 1077–1083.

Valentini, R., Epron, D., Angelis, P., Matteucci, G. and Dreyer, E. (1995) *In situ* estimation of net CO_2 assimilation, photosynthetic electron flow and photorespiration in Turkey oak (*Q. cerris* L.) leaves: diurnal cycles under different levels of water supply. *Plant, Cell & Environment*, 18, 631–640.

Wu, A., Hammer, G.L., Doherty, A., Caemmerer, S. von and **Farquhar, G.D.** (2019) Quantifying impacts of enhancing photosynthesis on crop yield. *Nature Plants*, 5, 380–388.

Wu, F., Sheng, P., Tan, J., Chen, X., Lu, G., Ma, W., Heng, Y., Lin, Q., Zhu, S., Wang, J., Wang, J., Guo, X., Zhang, X., Lei, C. and Wan, J. (2015) Plasma membrane receptor-like kinase leaf panicle 2 acts downstream of the DROUGHT AND SALT TOLERANCE transcription factor to regulate drought sensitivity in rice. *Journal of Experimental Botany*, 66, 271–281.

Xiong, D. and Flexas, J. (2018) Leaf economics spectrum in rice: leaf anatomical, biochemical, and physiological trait trade-offs. *Journal of Experimental Botany*, 69, 5599–5609.

Xiong, D., Flexas, J., Yu, T., Peng, S. and Huang, J. (2017) Leaf anatomy mediates coordination of leaf hydraulic conductance and mesophyll conductance to CO_2 in *Oryza*. *New Phytologist*, 213, 572–583.

Xiong, D. and Nadal, M. (2020) Linking water relations and hydraulics with photosynthesis. *Plant Journal*, 101, 800–815.

Xu, F., Wang, K., Yuan, W., Xu, W., Shuang, L., Kronzucker, H.J., Chen, G., Miao, R., Zhang, M., Ding, M., Xiao, L., Kai, L., Zhang, J. and Zhu, Y. (2019) Overexpression of rice aquaporin *OsPIP1;2* improves yield by enhancing mesophyll CO_2 conductance and phloem sucrose transport. *Journal of Experimental Botany*, 70, 671–681.

Yin, X., Struik, P.C., Romero, P., Harbinson, J., Evers, J.B., van der Putten, P.E.L. and Vos, J. (2009) Using combined measurements of gas exchange and chlorophyll fluorescence to estimate parameters of a biochemical C_3 photosynthesis model: a critical appraisal and a new integrated approach applied to leaves in a wheat (*Triticum aestivum*) canopy. *Plant, Cell & Environment*, 32, 448–464.

Yu, X., Peng, Y.H., Zhang, M.H., Shao, Y.J., Su, W.A. and Tang, Z.C. (2006) Water relations and an expression analysis of plasma membrane intrinsic proteins in sensitive and tolerant rice during chilling and recovery. *Cell Research*, 16, 599–608.

Figure legends

Figure 1. (a) Photograph of the representative plants, (b) tiller number and (c) plant height of wild type and *OsPIP* knockout lines. Plants were growing in paddy field in Sanya, Hainan. Photos and measurements were taken at 43 days after sowing. Different letters represent statistical significance (ANOVA, $P < 0.05$, n = 16-24).

Figure 2. (a) Photograph of the representative plants, (b) Tiller number and (c) plant height of wild type and *OsPIP* knockout lines. Photos were taken 56 days after sowing. Measurements were taken on plant growing in pot condition at 39, 57, 66 days after sowing in Wuhan. Means ± standard errors (SE). (ANOVA, $P < 0.05$, n = 10-16).

Figure 3. (a) Tiller number and (b) plant height of wild type and *OsPIP* knockout lines under filed and pot conditions. Measurements were taken on plants at about 40 days after sowing. Means ± standard errors (SE).

Figure 4. The photosynthetic rate (A), stomatal conductance (g_{sw}) and mesophyll conductance (g_m) of wild type and *OsPIP* knockout mutants at the PPFD of 1500 mol m^{-2} s^{-1} in Sanya (a, c, e) and Wuhan (b, d, f). Means ± standard error (SE). Different letters near the bars represent statistical significance (ANOVA, $P < 0.05$, n = 4-8).

Figure 5. CO_2 response curves of wild type and *OsPIP* knockout lines. A and C_i are net photosynthetic rate and intercellular CO_2 concentration, respectively. Measurements were conducted on plants grown under pot condition. The mean values were shown (n = 4-8).

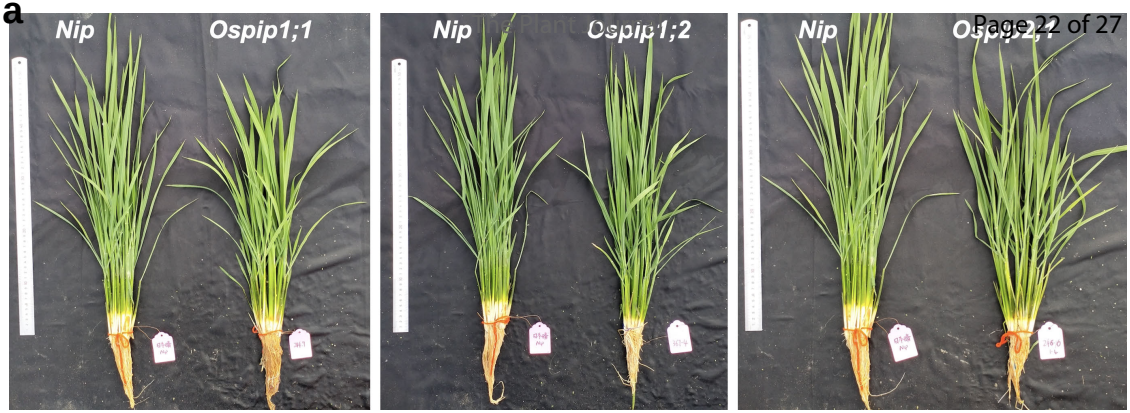
a
Nip
Ospip1;1
Nip
Ospip1;2
Nip
Ospip2;1

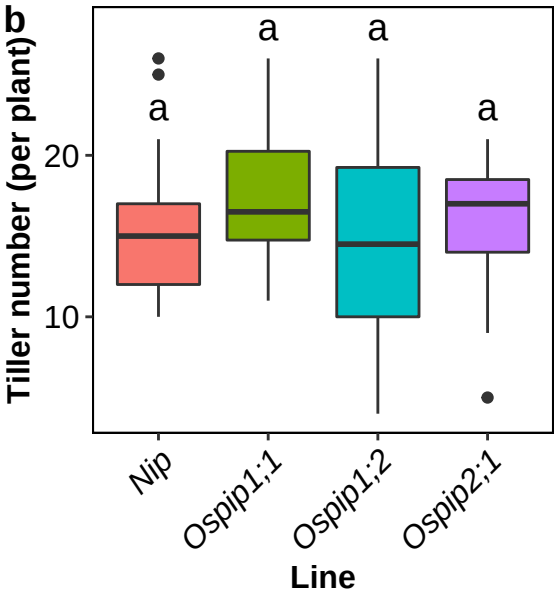
b
Tiller number (per plant)
20
10
a
a
a
a
Nip
Ospip1;1
Ospip1;2
Ospip2;1
Line

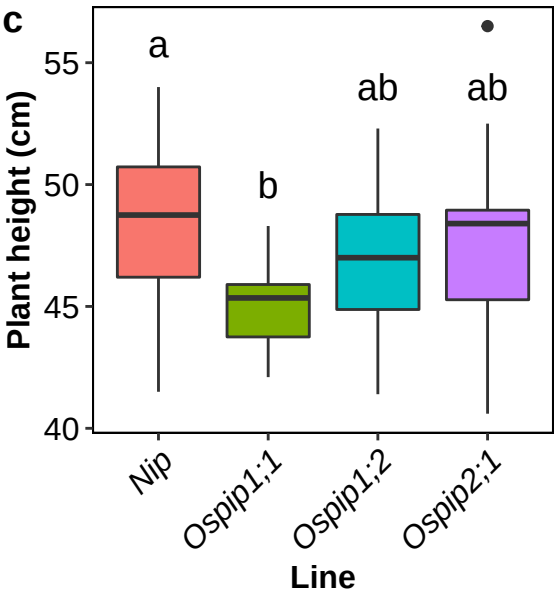
c
Plant height (cm)
55
50
45
40
a
b
ab
ab
Nip
Ospip1;1
Ospip1;2
Ospip2;1
Line


a
NiP Ospip1;1
NiP Ospip1;2
NiP Ospip2;1
b
The Plant Journal
Nip
Ospip1;1
Ospip1;2
Ospip2;1
Tiller number (per plant)
60
50
40
30
20
39
57
66
Day after sowing (day)
c
Plant height (cm)
90
80
70
60
50
39
57
66
Day after sowing (day)

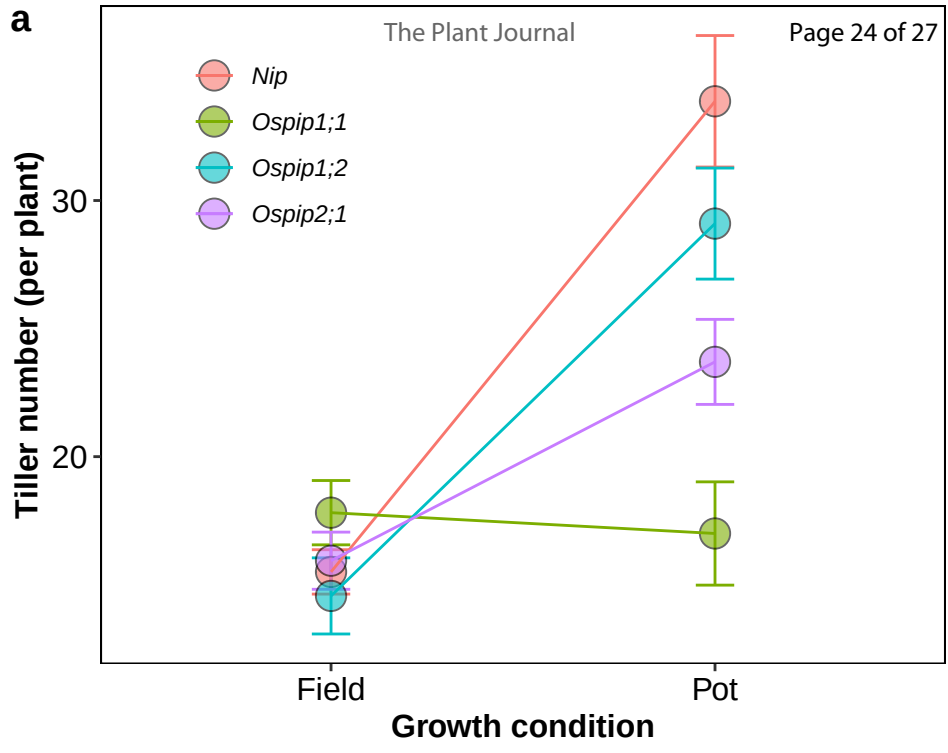
a
Nip
Ospip1;1
Ospip1;2
Ospip2;1
Tiller number (per plant)
30
20
Field
Pot
Growth condition

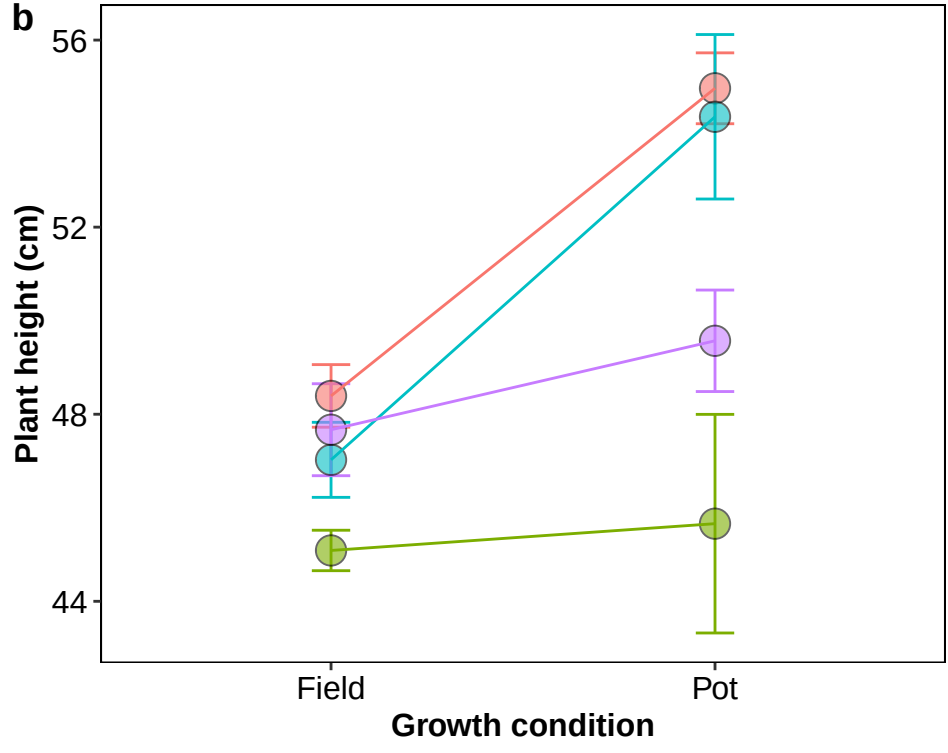
b
Plant height (cm)
56
52
48
44
Field
Pot
Growth condition

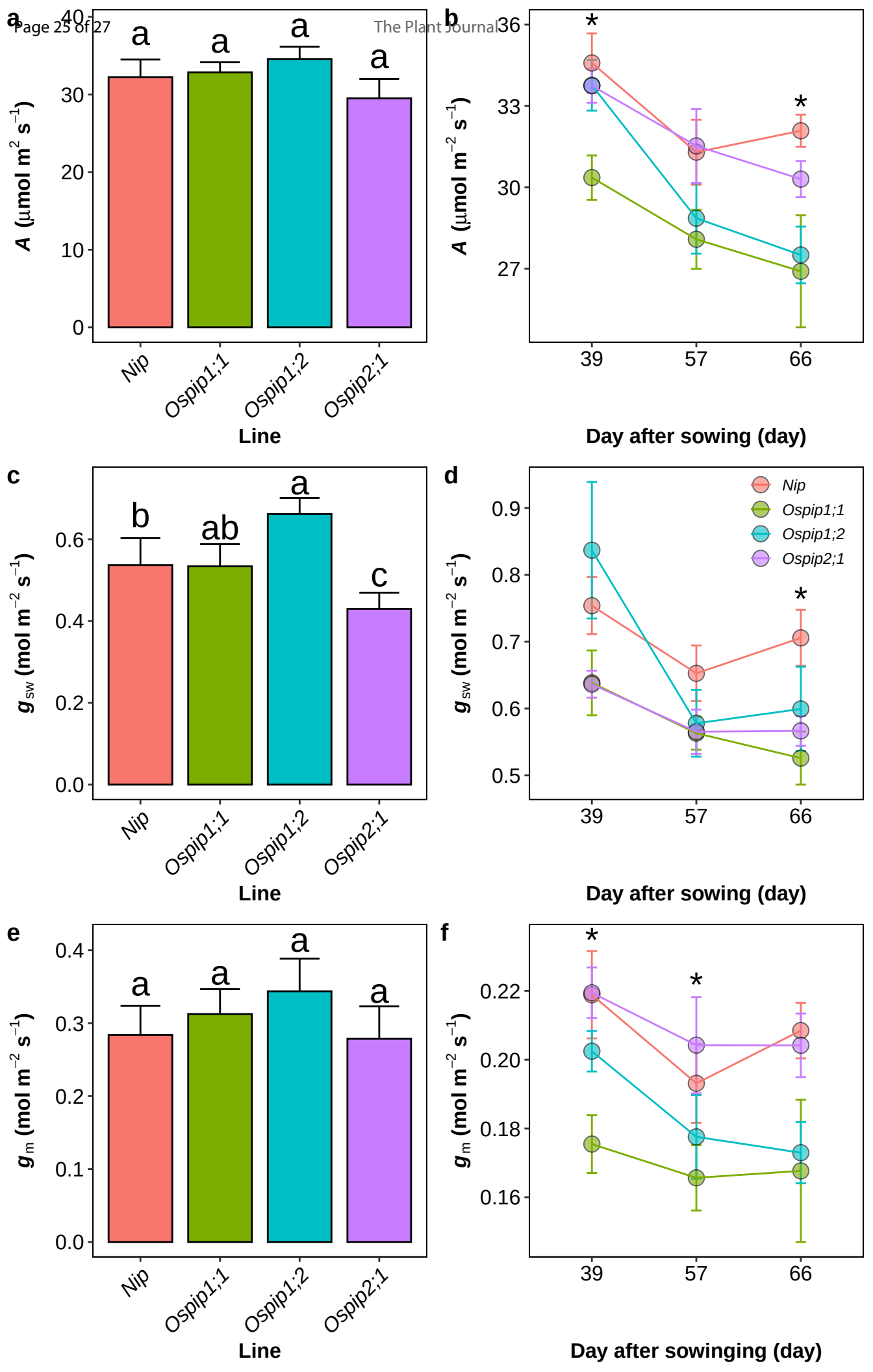
a
a
a
a
a
40
30
20
10
0
A (μmol m^{-2} s^{-1})
Nip
Ospip1;1
Ospip1;2
Ospip2;1
Line
b
*
*
36
33
30
27
A (μmol m^{-2} s^{-1})
39
57
66
Day after sowing (day)
c
b
ab
a
c
0.6
0.4
0.2
0.0
g_{sw} (mol m^{-2} s^{-1})
Nip
Ospip1;1
Ospip1;2
Ospip2;1
Line
d
Nip
Ospip1;1
Ospip1;2
Ospip2;1
*
0.9
0.8
0.7
0.6
0.5
g_{sw} (mol m^{-2} s^{-1})
39
57
66
Day after sowing (day)
e
a
a
a
a
0.4
0.3
0.2
0.1
0.0
g_m (mol m^{-2} s^{-1})
Nip
Ospip1;1
Ospip1;2
Ospip2;1
Line
f
*
*
0.22
0.20
0.18
0.16
g_m (mol m^{-2} s^{-1})
39
57
66
Day after sowinging (day)

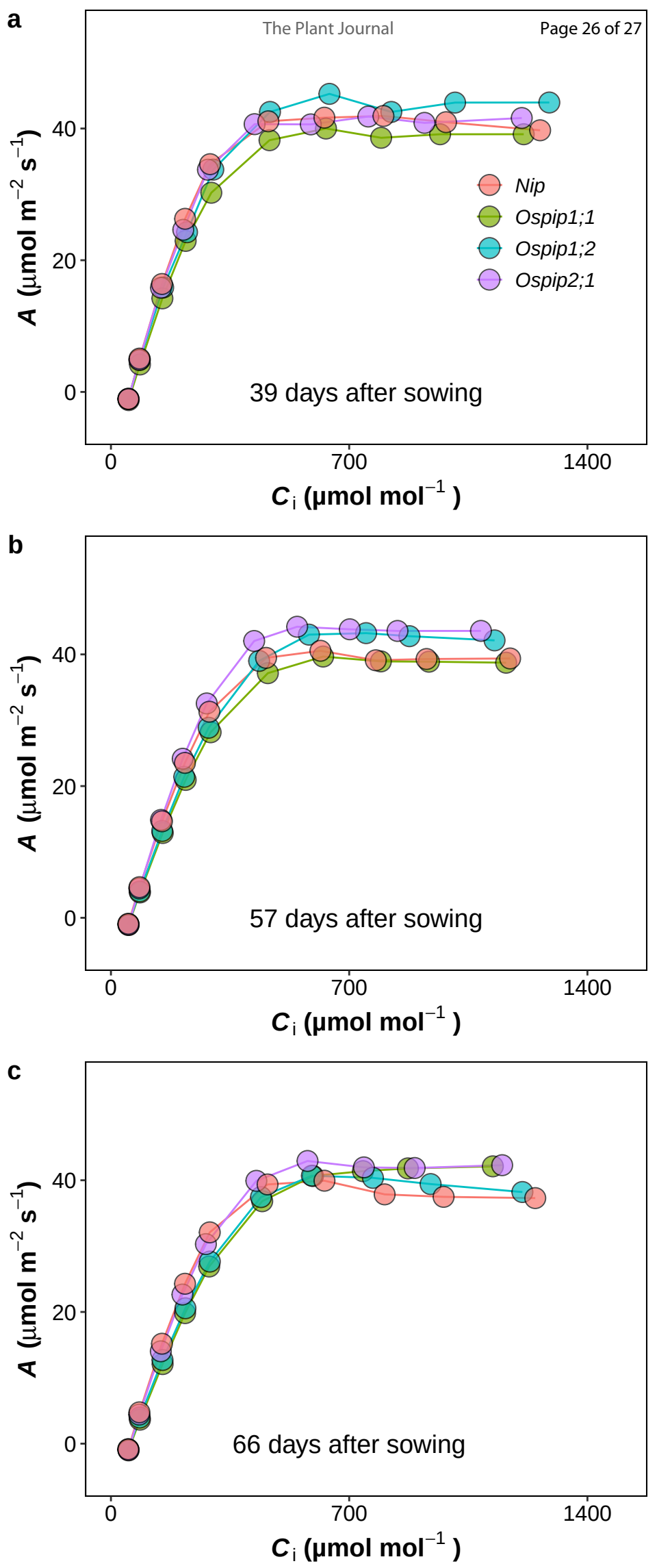
a
b
c
A (μmol m−2 s−1)
Ci (μmol mol−1)
0
20
40
0
700
1400
Nip
Ospip1;1
Ospip1;2
Ospip2;1
39 days after sowing
57 days after sowing
66 days after sowing

Significance statement

Differences in plant growth and photosynthetic performance between aquaporin knockout lines and the wild type were influenced by the growth stage of the plants and the planting conditions.